Z. Phys. B 97, 7–16 (1995)

ZEITSCHRIFT
FÜR PHYSIK B

Original Contributions

Electrostatic lattice coefficients and binding energy of orthorhombic $La_{2-x}Sr_xCuO_4$

Mario Birkholz[1], **Rainer Rudert**[2,*]

[1] Ingenieurbüro für Solartechnik, Offenbacher Strasse 7, D-14197 Berlin, Germany
[2] Max-Planck-Institut für Kolloid- und Grenzflächenforschung, Rudower Chaussee 5, D- 12489 Berlin, Germany

Received: 1 August 1994 / Revised version: 6 October 1994

Abstract. Three valency models for orthorhombic $La_{2-x}Sr_xCuO_4$ were investigated for increasing Sr concentrations x ($0 \leq x \leq 0.21$): 1. $Cu^{2+} \rightarrow Cu^{3+}$, 2. apex $O^{2-} \rightarrow O^-$ and 3. in-plane $O^{2-} \rightarrow O^-$. All calculations were done by using structural parameters valid for the temperature range from 10 to 22 K. We thereby calculated the electrostatic interaction energy which, next to ionization potentials and electron affinities, comprises a major of the binding energy E_B of crystals. Second-order effects were accounted for by calculating the strength of ionic dipole moments induced by crystal electric fields at relevant lattice sites. Their largest strengths are comparable to the dipole moment of the water molecule. Three out of five dipoles in $La_{2-x}Sr_xCuO_4$ vanish during the transition from the orthorhombic to the tetragonal phase. The binding energy differences between the different models suggest that the system is in a state of model 1. However, the differences are very small, being in the order of 0.3 to 0.76 eV at $x = 0.13$.

PACS: 61.50 Lt; 74.70.Vy

I. Introduction

The high-T_C superconducting cuprate compounds that have been synthesized and investigated since 1986 show high electrical conductivity in their normal state. Thus, they are often referred to as being metallic, see [1] for example as an introductory review of their physical properties. However, it has been recognized that a significant part of the crystal binding of these compounds must be understood in terms of the ionic model. Therefore, long-range electrostatic interactions are assumed to be an important factor in the cohesion of these solids. The ionic model concept has consequently been used to gain some insight into the nature of chemical bonding of these compounds and to understand some of their unusual and interesting properties.

In most cases, these investigations concentrate on first-order effects, i.e. interactions between electrical monopoles. Kondo, Asai and Nagai calculated the Coulomb energies in $YBa_2Cu_3O_{7-x}$ and related compounds in order to assess the consistency of certain charge assignments [2]. Later, Kondo used this approach for other HTSC compounds with even higher critical temperatures T_C [3]. Rushan and co-workers applied the concept of Watson-spheres to $YBa_2Cu_3O_{7-x}$ to identify the proper charge distribution [4]. This was also done by Cohen et al. for tetragonal and orthorhombic La_2CuO_4 to compare these results with those obtained from self-consistent charge density calculations [5]. Torrance and Metzger evaluated the difference between Coulomb potentials at the lattice site of copper and in-plane oxygen ions for the entire family of cuprate-based HTSC compounds [6], which was continued in greater detail by Ohta et al. [7]. Wang and co-workers demonstrated an interesting correlation for the difference between Madelung potentials of apical and planar oxygen ions varying in a comparable manner as $T_C(x)$ in $YBa_2Cu_3O_{7-x}$ [8]. Wright and Butler attempted to include the energy due to crystal field induced dipoles into their calculation of the Y-Ba-Cu-O-system. This was one of the very few studies takingsecond-order moments in HTSC compounds into consideration. However, in the case of $YBa_2Cu_3O_7$, they only obtained a saddle point and no minimum for the binding energy [9].

A previous publication [10] pointed out that the Coulomb energy accounts for the electrostatic interaction between charge distributions up to first order only, and that a more general electrostatic model should be used to describe heteropolar solids. This was outlined for dipoles that may occur on lattice sites whenever symmetry allows for a non-vanishing crystal electric field that cause a polarization of the ion. Infinite lattice sums were introduced for the potential and fields of monopoles and dipoles, with

* *Present address:* Bundesanstalt für Materialprüfung und -forschung, Rudower Chaussee 5, D-12489 Berlin, Germany

the Madelung constant being the first term in the Taylor expansion of the electrostatic interaction within a solid. These sums, which yield definite values for every crystallographic structure, have been named electrostatic lattice coefficients. With their help an expression for the binding energy of a crystal was formulated. The energy due to induced dipoles was thereby found to be always negative, i.e. the dipoles enhance crystal binding.

In this work, the first and second-order electrostatic lattice coefficients of orthorhombic $La_{2-x}Sr_xCuO_4$ for $0.0 \leq x \leq 0.21$ and $T \approx 16\,K$ will be presented using different assignments of ionic charges. Dipole moments induced by the crystal electric field will be calculated with the help of ionic polarizabilities. We will attempt to determine which sort of ion is oxidized with increasing Sr concentration or doping rate x. It is the aim of this work to decide by a minimization of the binding energy, whether holes are favoured to reside on copper ions, apical or in-plane oxygens. We hope to obtain improved results by including second-order effects, which – to our knowledge – have not been considered so far.

II. Method

The concept of electrostatic lattice coefficients has been outlined up to second order in [10]. It was argued that the electrostatic interaction energy E_{el} of the crystal can be expanded in a Taylor series, in which the first two terms account for the interaction of charges q_i with potentials (i) of other charges and (ii) of dipoles p_j. The latter depend on symmetry and vanish at lattice sites of certain symmetry point groups. Infinite lattice sums that are to extend over potentials of monopoles and dipoles were abbreviated α^m and α^d, with α^m being the known Madelung constant. Those that account for fields of point charges and dipoles were labelled β^m and β^d. These electrostatic lattice coefficients are pure geometric quantities that can be calculated if precise structural parameters are available.

Most superconducting cuprates are orthorhombic and may be regarded to be derived from so-called parent compounds, the latter being non-superconducting, but electrically isolating. A common feature of all superconducting cuprates is that their CuO_2 layers are oriented perpendicular with respect to the crystallographic c-axis of the unit cell. In $La_{2-x}CuO_4$ these layers are separated by two LaO layers. Sr ions in $La_{2-x}Sr_xCuO_4$ were found to be randomly distributed over La sites [11]. The symbol LS will therefore be used in the following to indicate a lattice site occupied by either an La or an Sr ion. Cu ions are octahedrally coordinated to two apical oxygen atoms of the LS-O layer, abbreviated as O(A), and to four in-plane oxygens O(P), see Fig. 1. In the orthorhombic phase O(P) and Cu ions do not constitute a perfectly planar layer. Instead the oxygen layer is slightly buckled below and above the copper plane. The lattice sites for the four different ions in the *Bmab* setting of the unit cell are listed in Table 1 and are shown in Fig. 1.

Crystals of $La_{2-x}Sr_xCuO_4$, abbreviated LSCO in the following exhibit two important modifications. One is a high temperature tetragonal phase (HTT), which contains two formula units per unit cell, $Z = 2$, and the other is a low temperature orthorhombic phase (LTO) with $Z = 4$. The structural phase transition temperature T_{t-0} of about 530 K for $x = 0$ [12] decreases with increasing Sr concentration x and reaches zero for $x \approx 0.21$ [13]. Our calculations will be based upon three points within the (T, x) phase diagram: $x = 0, 0.13$ and 0.21. This is always calculated at a temperature T of about 16 K, since this is the most interesting range with respect to the superconducting properties of the compound. The first two points were taken from structural parameters previously given in the work of Jorgensen et al. and Braden

Table 1. Crystallographic unit cell and dipole unit vectors n of the ions in orthorhombic $La_{2-x}Sr_xCuO_4$. The unit cell is given in space group *Bmab*. It contains two of the charge and dipole configuration given in the Table, with the second one being shifted by the translation $\tau = (\frac{1}{2}\,0\,\frac{1}{2})$. The unit vectors n_b of O(A) and LS point into opposite directions since the signs of their y coordinates are different, see Table 2. The actual dipole vectors are obtained by multiplying with the dipole strength μ_j as given in Tables 5–7

Cu	000	$0\frac{1}{2}\frac{1}{2}$		
La, Sr	0 y z	$0\,\bar{y}\,\bar{z}$	$\frac{1}{2},\frac{1}{2}-y,z$	$\frac{1}{2},\frac{1}{2}+y,\bar{z}$
n_b(LS)	(0 1 0)	$(0\,\bar{1}\,0)$	$(0\,\bar{1}\,0)$	(0 1 0)
n_c(LS)	(0 0 1)	$(0\,0\,\bar{1})$	(0 0 1)	$(0\,0\,\bar{1})$
O(A)	0 y z	$0\,\bar{y}\,\bar{z}$	$\frac{1}{2},\frac{1}{2}-y,z$	$\frac{1}{2},\frac{1}{2}+y,\bar{z}$
n_b(O(A))	$(0\,\bar{1}\,0)$	(0 1 0)	(0 1 0)	$(0\,\bar{1}\,0)$
n_c(O(A))	(0 0 1)	$(0\,0\,\bar{1})$	(0 0 1)	$(0\,0\,\bar{1})$
O(P)	$\frac{1}{4}\frac{1}{4}z$	$\frac{3}{4}\frac{3}{4}\bar{z}$	$\frac{3}{4}\frac{1}{4}z$	$\frac{1}{4}\frac{3}{4}\bar{z}$
n_c(O(P))	(0 0 1)	$(0\,0\,\bar{1})$	(0 0 1)	$(0\,0\,\bar{1})$

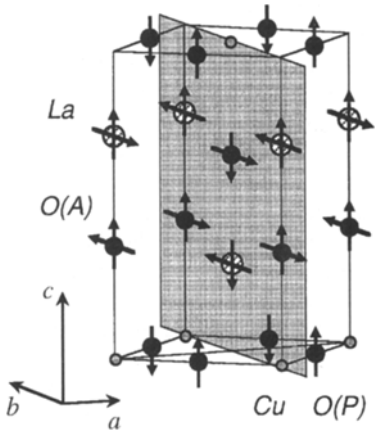

Fig. 1. Structure of orthorhombic La_2CuO_4. For simplification, the picture only displays the unit cell of the HTT phase up to a height of $c/2$. The orientations of cell edges of the LTO phase in the *Bmab* setting are shown. The a and b axes of the orthorhombic cell are directed along the diagonals of the basal plane of the tetragonal phase. The bc plane of the LTO cell has been emphasized. Dipole unit vectors of the ions as given in the figure follow from the site symmetry and the rotation operations between equivalent sites. While two independent dipole components occur within the bc plane for La and O(A), there is only one dipolar degree of freedom for O(P) in direction of the c-axis. No dipole moments can be induced on Cu ions, since they reside on positions where crystal electrical fields are forbidden by symmetry

et al. [14, 15]. The third one was obtained by an extrapolation as follows.

The data set of Jorgensen et al. ($x = 0.0$) was obtained at $T = 10$ K, while that of Braden et al. ($x = 0.13$) was determined for 22 K. The latter group also analyzed the structure of LSCO at the phase point $(T, x) = (50, 0)$ [15]. This data set did not significantly deviate from the one measured by Jorgensen et al. at 10 K. We conclude that the structural parameters of LSCO are stronger influenced by the doping rate than by small temperature changes. Therefore, the two data sets for $x = 0$ and 0.13 are assumed to be valid for the temperature range from 10 to 22 K, which is abbreviated as $T \approx 16$ K in the following.

The through and extensive study performed by Braden et al. [15] allows for an interpolation of the cell edge b for varying x. This quantity is found to exhibit a linear dependency upon x for $T = 295$ K, which even applies for crossing the phase boundary from LTO $\rightarrow$ HTT. We assumed this rule to be valid at 16 K also, and extrapolated $b(x)$ as given for $x = 0$ and 0.13 up to 0.21. At this point the two cell constants a and b must become equal according to Takagi et al. [13]. Consequently, the first two parameters have been determined for LSCO at $x = 0.21$: $a = b = 5.3131$ Å. The same linear extrapolation of data for $x = 0$ and 0.13 was applied upon the third cell edge, yielding $c = 13.2324$ Å for $(T, x) = (16, 0.21)$. The tetragonal phase is characterized by the absence of tilting of CuO_6 octahedrons. 4-fold rotation axes arise for all ions which causes three of the positional parameters to vanish: $y(\mathrm{LS}) = y(\mathrm{O(A)}) = z(\mathrm{O(P)}) = 0$. Now, only the heights of LS and O(A) ions in the unit cell must still be extrapolated. Both are found to depend linearly on the doping rate x at 295 K [15]. We again extrapolated the figures of Jorgensen et al. and Braden et al. and, finally, the last two parameters of the LSCO structure at the phase point $(T, x) = (16, 0.21)$ were determined. All the ions' coordinates used in this work are compiled in Table 2.

An ongoing discussion about the oxidation state of copper and oxygen ions exists because of the distribution of charge carries in CuO_2 layers. However, there is a consensus that the assignment of charges in La_2CuO_4 should be Cu^{2+}, La^{3+} and O^{2-}. Problem arise with the incorporation of x mole Sr atoms. If the valency of the substitute is assumed to be Sr^{2+}, another ion must be oxidized to maintain the crystal's charge neutrality. To answer this question, three valency models were investigated, which assume that holes introduced by doping are localised on copper ions (Model 1), apex oxygens (Model 2) or in-plane oxygens (Model 3), respectively. In all models we assume that the charges of one sort of ions $q_i = z_i e$ are randomly distributed over the ith lattice sites, as has been determined experimentally [11]. For example, the probability that the LS site will be occupied by an La^{3+} ion is $(2 - x)/2$, as compared to the complementary probability $x/2$ for an Sr^{2+} ion. Due to this distribution the mean charge of that site becomes $(3 - x/2)$, which will be the same in all three models. In model 1 we then assume that there are as many Cu^{3+} as Sr^{2+} in the lattice, leading to $q_{Cu} = (2 + x)$ for this model. The average of the charges of O(A) and O(P) equal $-(2 - x/2)$ for model 2 or 3, respectively. The x-dependent functions of the mean charges for all three models are given in Table 3. Although LSCO can be synthesized with a strong oxygen deficit [16], only the stoichiometric compound will be considered here.

Dipole moments will be induced in those ions where the point symmetry of the lattice site allows for a non-vanishing crystal electric field [10]. In the case of orthorhombic LSCO, the problem is easily solved for the Cu and the O(P) site. Copper ions reside on positions of point group C_{2h} in Schönflies' notation ($2/m$ in terms of the international notation), and are subjected to an inversional symmetry where any electric field or dipole vector must equal its negative and must therefore set to be zero. O(P) ions are located on a 2-fold rotation axis (point group C_2 or 2) which is parallel to the unit cell's c-axis. A non-vanishing dipole vector $p_C(\mathrm{O(P)})$ is allowed at such a site, which is oriented along the symmetry axis with only one independent component. A priori its strength is unknown, but we assign a dipole unit vector $n_C(\mathrm{O(P)})$ to that ion.

The relevant symmetry element for LS and O(A) ions, however, is not an axis of rotation but a mirror plane being parallel to the unit cell's bc face, see Fig. 1. The point group of the lattice sites is C_{1h} (or m), and both ions have *two* independent dipole components, the unit vectors of which will be abbreviated as n_b and n_c in the following. The actual dipole vector, of course, is a linear combination of the two spatial components. It should be emphasized that two second-order moments occur for each ion, p_b and

Table 2. Structure parameter of orthorhombic $La_{2-x}Sr_xCuO_4$ for different Sr concentration x as they were used for the calculation of the electrostatic lattice coefficients. The data sets for $x = 0$ and 0.13 have been determined by neutron diffraction, while that for 0.21 has been estimated as described in the text. w and E_0 stand for the cube root of the volume of the unit cell and the energy unit of the system

x	0.0	0.13	0.21
a/Å	5.3349	5.3288	5.3131
b/Å	5.4204	5.3540	5.3131
c/Å	13.1072	13.1847	13.2324
w/Å	7.2370	7.2187	7.2019
$y(\mathrm{LS})/b$	0.0092	0.00506	0
$z(\mathrm{LS})/c$	0.3616	0.36077	0.36026
$y(\mathrm{O(A)})/b$	−0.0410	−0.02447	0
$z(\mathrm{O(A)})/c$	0.1841	0.18227	0.18114
$z(\mathrm{O(P)})/c$	0.0087	0.00511	0
E_0/eV	1.9897	1.9948	1.9994
Determined at T/K	10	22	ca. 16
Method	Neutr. Diff.	Neutr. Diff.	Estimated
Reference	[14]	[15]	this work

Table 3. Ionic charges as used for the different valency models, $z_i(x) = z_i(0) + s(z_i)x$, being linear functions of the Sr concentration x

Ion i	Cu 1	La, Sr 2	O(A) 3	O(P) 4
$z_i(0)$	2	3	−2	−2
$s(z_i)$ M1	1	−0.5	0	0
$s(z_i)$ M2	0	−0.5	0.5	0
$s(z_i)$ M3	0	−0.5	0	0.5

p_c, in contrast to the monopoles that have only one degree of freedom. Whereas z_i, $i = 1, 2, 3, 4$ stands for the charges of the Cu, LS, O(A) and O(P) ions, the numbering of the set of dipoles is completely different. Their unit vectors are abbreviated by the sequence n_j with $j = 1, 2, 3, 4, 5$ to indicate n_b(LS), n_c(LS), n_b(O(A)), n_c(O(A)), and n_c(O(P)), see Table 1. Unit vectors were assigned in accordance with the symmetry operations of the unit cell, i.e. unit vectors on equivalent lattice sites are related by the appropriate rotation matrices.

The foregoing arguments are only valid for the orthorhombic phase of LSCO. During the transition to the HTT phase, the buckling of CuO_2 layers vanishes, thereby causing the dipole component of O(P) ions to disappear. Moreover, LS and O(A) positions become sites of higher symmetry, which is accompained by a change to point group C_{4v} (4 *mm*). This allows for only one dipole moment component along the crystallographic *c* direction (see Table 1, [10]). We conclude that n_b(LS), n_b(O(A)) and n_c(O(P)) all become zero in the HTT phase. Instead of five independent dipole components, only two remain in tetragonal LSCO, namely n_c(LS), and n_c(O(A)). The occurrence of induced dipoles for all but for Cu ions follows the prediction of [17]. This work argued that highly polarizable ions will preferably reside on dipole-allowed lattice sites.

All electrostatic lattice coefficients will be calculated by using distances normalized with respect to the cube root of the cell volume, which is the geometric mean of the crystallographic axes $w = \sqrt[3]{abc}$ in the case considered here. This should be kept in mind when comparing values of Madelung constants α^m with those from other works, in which the smallest bond length is often taken as unit distance. Accordingly, the energy unit of the system becomes $E_0 = e^2/4\pi\varepsilon_0 w$, which can be expressed as $2\,Ry\;a_0/w$, with a_0 being Bohr's radius. For instance, at $T = 22$ K and $x = 0.13$ the unit length is found to be $w = 7.2187$ Å yielding $E_0 = 1.9948$ eV.

The strengths of the dipoles p are assumed to be proportional to that of the exciting electric field F, $p = 4\pi\varepsilon_0\kappa F$, with κ being the ion's polarizability. If all β coefficients are known, the dipoles may be obtained from the system of equations

$$\sum_{k=1}^{5}\left(\delta_{jk}\frac{w^3}{\kappa_j} - \beta_{jk}^d\right)\mu_k = \beta_j^m \tag{1}$$

with μ_j being the normalized dipole strength p_j/ew. We used the polarizabilities κ given in [18] for La^{3+} and Sr^{2+} (1.41 and 1.01 Å^3, respectively). The polarizability of LS ions in the investigated x range was set to be the weighted average of both ions, $[(2-x)\kappa(La^{3+}) + x\kappa(Sr^{2+})]/2$. For oxygen with a doubly negative charge, a polarizability of 2.86 Å^3 was used. This figure can be deduced from measurements of the high-frequency dielectric constant ε_∞ of cubic SrO [19]. However, values for $\kappa(O^{2-})$ vary by approximately 40% in different compounds [20–23], and additional studies will be required to determine the precise value of $\kappa(O^{2-})$ in LSCO. Since we were unable to find any indication of the polarizability of O^- in the literature, it was estimated to be roughly $\kappa(O^-) = 0.6\times\kappa(O^{2-}) + 0.4\times\kappa(O) = 2.04$ Å^3, with $\kappa(O) = 0.8$ Å^3 according to Ref. [24]. It may be concluded that metal polarizabilities are more reliable, whereas $\kappa(O^-)$ and $\kappa(O^{2-})$ are only estimates. The polarizability κ_j of all ions and valency models are compiled in Table 4. The values are constant or vary linearly with the doping rate.

Finally, we may describe the binding energy E_B of LSCO as the sum of the ionization processes E_I, Coulomb interaction E_C, polarization energy E_p and terms reflecting the repulsion of core electrons E_r, van der Waals attraction E_{vdW} and thermal vibrations E_{tv}

$$E_B = E_I + E_C + E_p + E_r + E_{vdW} + E_{tv} \tag{2}$$

If there are K_i ions of *i*.th sort in the unit cell, the first three terms may be comprised by an energy parameter E as follows

$$E = E_I + E_C + E_p$$
$$= \sum_{i=1}^{4}\frac{K_i}{Z}\left[I_i - A_i + \frac{E_0}{2}z_i\left\{\alpha_i^m + \sum_{j=1}^{5}\mu_j\alpha_{ij}^d\right\}\right] \tag{3}$$

with I_i and A_i representing the ionization energy necessary to transform the atom to the proper ion (ionization potentials and electrons affinities) [10].

To decide which charge distribution will actually be applied in LSCO, we used the ansatz

$$\left.\frac{\partial E_B}{\partial z_i}\right|_{\sum K_i z_i = 0} = 0 \tag{4}$$

This indicates that the system will minimize its energy with respect to the proper distribution of charges. Since the ions can only bear integer numbers of charges, (4) forces us to compare the binding energies of the different models. With some justification it may be assumed that the three last terms in (2), $E_r + E_{vdW} + E_{tv}$, are the same for all three valency models. Instead of E_B we therefore will compare the energy parameters E in the following chapter, with the smallest E accounting for the valency model actually applied in $La_{2-x}Sr_xCuO_4$. The major uncertainty is caused by the imprecise value for the second electron affinity of oxygen, A_2(O), which different investigators have used as -6.7, -7, -8.1 and -8.75 eV, respectively [2, 3, 6, 24, 25]. We utilized a mean value of -7.7 eV.

Our basic approach can be criticized, because it disregards such collective effects of the electronic ensemble as antiferromagnetism occurring in La_2CuO_4 and the superconductivity observed for $0.06 \lesssim x \lesssim 0.25$. Both phenomena can cause additional summands E_{AF} and E_{SC},

Table 4. Ionic polarizabilities κ in units of Å^3 for the different valency models, depending linearly upon the doping rate, $\kappa_j(x) = \kappa_j(0) + s(\kappa_i)x$

Dipole j	p_b(LS) 1	p_c(LS) 2	p_b(O(A)) 3	p_c(O(A)) 4	p_c(O(P)) 5
$\kappa_j(0)$	1.41	1.41	2.86	2.86	2.86
$s(\kappa_j)$ M1	−0.2	−0.2	0	0	0
$s(\kappa_j)$ M2	−0.2	−0.2	−0.4	−0.4	0
$s(\kappa_j)$ M3	−0.2	−0.2	0	0	−0.4

which must be included in the binding energy E_B. However, both terms are much smaller than the dominant lattice energy. Magnetic interactions can be estimated [26] from $T_N \approx 300$ K of La_2CuO_4 to account for 25 meV maximally, and E_{SC} determined from specific heat measurements is even less than 1 meV per formula unit [27]. Therefore, when attempting to determine which charge assignment is actually taken by the system, the influence of these effects is assumed to be small and will be neglected.

III. Results and discussion

All electrostatic lattice coefficients were calculated by a fast converging direct-lattice summation procedure. For the calculation of α^m and β^m, point charge clusters without higher electrostatic moments were summed as first done by Evjen [28] and later optimized, see for instanc Ref. [29]. α^d and β^d coefficients were obtained by generalizing this method to clusters of dipoles [30]. The results for Sr concentrations of $x = 0$, 0.13 and 0.21 are given in Tables 5–7 and are valid for $T \approx 16$ K. The complexity of the ionic interactions in and the physics of LSCO is clearly illustrated by the size of these tables. However, compared to other HTSC cuprates the structure of $La_{2-x}Sr_xCuO_4$ is relatively simple.

We shall first consider the results obtained for La_2CuO_4, see Table 5. Regarding the Coulomb or monopole potentials, α_i^m or $V_i^m = E_0\alpha_i^m$, at the metal sites, $i = 1$ and the one of La is seen to be smaller than that of Cu, $\alpha_2^m < \alpha_1^m$. The energy gain of the system is maximized with a charge of +3 instead of +2 at the La position. The Coulomb potentials are therefore concluded to give consistent results for the metal ions and to justify the charge assignment of La^{3+} and Cu^{2+} in La_2CuO_4. In the case of

Table 5. Electrostatic lattice coefficients α_i^m, α_{ij}^d, β_i^m, β_{ij}^d and derived quantities as dipole strengths μ_j and dipole potentials for the four ionic positions and five induced dipoles for La_2CuO_4, calculated with structural parameters as measured at $T = 10$ K. Dipoles μ_j and Madelung and dipole potentials, α_i^m and $\Sigma\mu_j\alpha_{ij}^d$, are given in units of 10^{-2} *ew* and E_0/e, respectively, accounting for $E_0 = 1.9897$ eV at $x = 0$

$x=0$	Cu	La, Sr	O(A)	O(P)		p_b(LS)	p_c(LS)	p_b(O(A))	p_c(O(A))	p_c(O(P))
i	1	2	3	4	j	1	2	3	4	5
α_i^m	−14.0485	−14.1432	10.0984	10.7620	β_j^m	1.5051	−0.7654	−3.4817	−4.3724	−0.4301
$j=1$	0.2093	0.1750	2.1842	−1.0645		7.8752	0.0431	−66.881	20.083	75.025
$j=2$	13.8346	−1.5698	−13.8690	18.0488		0.0431	−58.406	−1.001	127.116	11.2815
α_{ij}^d $j=3$	−0.7816	1.4403	0.4476	−0.4188	β_{ij}^d	−66.881	−1.001	33.614	3.655	35.810
$j=4$	−16.1442	3.9996	6.9999	−11.2588		20.083	127.116	3.655	−27.504	−13.926
$j=5$	−3.4708	0.5360	0.2995	−1.4460		75.025	11.2815	35.810	−13.926	15.568
$\Sigma\mu_j\alpha_{ij}^d$	0.4685	−0.2043	−0.0272	0.1452	μ_j	1.287	−1.823	−4.774	−4.067	−0.695

Table 6. Electrostatic lattice coefficients α_i^m, α_{ij}^d, β_{ij}^d and dipole strengths μ_j for $La_{1.87}Sr_{0.13}CuO_4$ at $T = 22$ K for the three different valency models M1–M3 as explained in the text. Dipole strengths in units of 10^{-2} *ew*

$x=0.13$	Cu	La, Sr	O(A)	O(P)			p_b(LS)	p_c(LS)	p_b(O(A))	p_c(O(A))	p_c(O(P))
i	1	2	3	4		j	1	2	3	4	5
M1	−14.7018	−13.8192	10.0534	10.8456		M1	0.874	−1.425	−2.926	−3.327	−0.490
α_i^m M2	−14.3441	−13.7490	9.8916	10.4964	μ_j	M2	0.773	−1.144	−2.894	−3.999	−0.611
M3	−14.0172	−13.7905	10.0312	10.4443		M3	0.870	−1.654	−2.966	−3.701	−0.549
$j=1$	0.1140	0.0975	1.3532	−0.6248			7.694	0.0071	−68.306	11.420	73.330
$j=2$	14.0965	−1.7768	−13.5884	18.2781			0.0071	−58.960	−0.452	128.540	6.296
α_{ij}^d $j=3$	−0.4718	0.8942	0.2867	−0.2600		β_{ij}^d	−68.306	−0.452	31.971	2.158	37.082
$j=4$	−16.6647	4.1032	7.1354	−11.8067			11.420	128.540	2.158	−30.505	−8.246
$j=5$	−2.1018	0.3680	0.1689	−0.8967			73.330	6.296	37.082	−8.246	18.004

Table 7. Electrostatic lattice coefficients α_i^m, α_{ij}^d, β_{ij}^d and dipole strengths μ_j for $La_{1.79}Sr_{0.21}CuO_4$ at $T = 16$ K for the three different valency models M1–M3 as explained in the text. Dipole strengths in units of 10^{-2} *ew*

$x=0.21$	Cu	La, Sr	O(A)	O(P)			p_c(LS)	p_c(O(A))
i	1	2	3	4		j	2	4
M1	−15.1060	−13.6190	10.0318	10.8979		M1	−1.151	−2.805
α_i^m M2	−14.5326	−13.5036	9.7687	10.3251	μ_j	M2	−0.708	−3.913
M3	−13.9958	−13.5738	9.9958	10.2476		M3	−1.515	−3.403
$j=2$	14.2872	−1.9106	−13.4025	18.4295			−59.400	129.254
α_{ij}^d					β_{ij}^d			
$j=4$	−16.9852	4.1329	7.2135	−12.1589			129.254	−32.528

the oxygen lattice sites, negative charges are revealed to be more stable at in-plane than at apex position, $(-2)\alpha_4^m < (-2)\alpha_3^m$.

The 20 α^d coefficients that account for the interaction of four charges with five dipoles are found to be more significant for dipoles oriented along the c-axis, see the large values of α_{i2}^d and α_{i4}^d. The p_c dipole components of La and O(A) are therefore much stronger coupled to the ions than other dipoles, because most of the α_{ij}^d coefficients with $j = 1, 3, 5$ deviate only slightly from zero. For the transition to the tetragonal phase at $x = 0.21$ the latter components of the α^d matrix will vanish, since point symmetries at the ionic sites forbid the formation of dipoles along the b-axis or out of the basal plane of the unit cell. Moreover, a careful analysis of the most relevant α_{i2}^d and α_{i4}^d reveals that the interaction with p_c dipoles is smallest for La ions as mediated by α_{2j}^d coefficients. In other words, the structure of La_2CuO_4 favours the charge-dipole interaction between the ions that constitute the CuO_6 octahedron and the two strong dipoles along the c axis.

For completeness we also present the β^m coefficients in Table 5, although they can be calculated [10] according to the relation

$$\beta_j^m = -\sum_{i=1}^{4} \frac{K_i}{L_j} z_i \alpha_{ij}^d \tag{5}$$

Both β^m and α^d account for the interaction between charges and dipoles in the crystal lattice, describing the same interaction from two different points of view. From the standpoint of dipoles, p_b and p_c of O(A) are seen to be most significantly coupled to the ionic charges via their large β^m coefficients. This is reasonable, because the system can gain the most energy by this choice due to the higher polarizability of oxygen ions compared to lanthanum ions and because of the larger number of dipole components for apex oxygens compared to in-plane oxygens.

In Table 5 the β_{ij}^d matrix is seen to be symmetric, as is the dipole-dipole interaction it describes. The strongest component, β_{24}^d, accounts for the coupling between p_c dipoles of La and O(A). This again emphasizes the dominant role they play in the structure and binding of La_2CuO_4. The relevant term for the associated energy, β_{24}^d/w^3, is found to be stronger by a factor of 20 compared for instance to β^d/a^3 of pyrite [31]. The latter is a measure for the interaction energy between the sulfur dipoles in the pyrite lattice. The reason for the large β^d coefficient in La_2CuO_4 is the anti-parallel orientation of the dipole unit vectors n_c(La) and n_c(O(A)) within the La-O(A) layer, which is known to maximize this orientation-sensitive interaction. Due to the same reason, β_{13}^d which is responsible for the coupling of n_b(La) and n_b(O(A)), is identified to be one of the largests component of the β_{ij}^d matrix. At the phase transition LTO $\rightarrow$ HTT all components except for β_{24}^d, β_{44}^d and β_{22}^d will vanish.

Apart from the electrostatic lattice coefficients, Table 5 also specifies the dipoles strengths μ_j as induced by the crystal electrical fields in La_2CuO_4. These are calculated according to (1) and are given in units of 10^{-2} ew. The absolute strength of the dipoles p_j in units of eÅ is obtained by multiplying with w, see Table 2 (1 eÅ = 4.8 Deb = 1.602×10^{-29} Cm). When comparing these values with other figures, one should keep in mind that the dipole moment of the water molecule amounts to 0.38 eÅ [32], while that of dimers of alkali halides in the gas phase range from 1.2 to 2.5 eÅ [33]. In FeS_2 the induced dipole at the sulfur lattice site (0.768 eÅ [31]) is almost twice as large as the largest moment of La_2CuO_4, namely $p(O(A)) = (p_b^2 + p_c^2)^{1/2} = 0.45$ eÅ. Since the polarizability κ of the sulfur ion is roughly twice as large as that of oxygen, we conclude that the strength of the inducing crystal electric fields is comparable in both compounds, i.e. in the range of 10^{10} Vm^{-1}.

Another finding is that the signs of β^m coefficients and dipoles μ are equal, meaning that the dipoles are oriented along the same direction as are the electric fields due to monopoles. [10] distinguished between dipole strengths ϕ induced by the charges, where $\phi_j = \kappa_j \beta_j^m / w^3$, and dipole strengths induced by combined monopole and dipole fields, given in (1). A thorough analysis of all five dipole components of La_2CuO_4 shows that the inequality $|\phi_j| < |\mu_j|$ holds, i.e. all charge-induced dipoles are enhanced by the recursive effect of dipole-dipole interaction. The increase in dipole moments due to the field of other dipoles is 2 to 6-fold – an enormous enhancement of dipole strength. Furthermore, the b-components of La and O(A) dipoles are, remarkably, on the same order of magnitude as are the components along the c direction. This is unexpected, since spatial deviation from the c-axis is very small, i.e. in the order of 10^{-2} Å. Both ions are positioned on this axis in the tetragonal phase, thereby causing the p_b components to vanish. Consequently, they both were expected to be rather small in the LTO phase.

Finally, Table 5 presents the dipole potentials that occur at ions' sites attributable to second moments, $V_i^d = E_0 \sum \mu_j \alpha_{ij}^d$. They reach a maximum share of 3.3% of the Coulomb potentials, which justifies neglecting them in many cases. Under some circumstances, however, their influence can be significant and they may tip the scales. In our case, the potentials at the metal lattice sites were influenced in such a way that the distinction between them was increased, i.e. a charge of +3 is even more stabilized at La sites compared to Cu sites. This is visualized in Figs. 2a and 6a, where the site potentials of Cu and La can be seen to increase from 0.2 to 1.5 eV for $x = 0$ if dipole effects are included. The consistency of the charge assignment of La^{3+} and Cu^{2+} as stated above, is underlined by the inclusion of dipole potentials. The same holds true for the oxygen sites, where the distinction is also increased: $V_{O(A)}^m + V_{O(A)}^d < V_{O(A)}^m < V_{O(P)}^m < V_{O(P)}^m + V_{O(P)}^d$, see Figs. 2b and 6b. From the latter argument it can be concluded that, if electrons are depleted from oxygen sites for $x \neq 0$, it will be more favorable to oxidize O(A) than O(P).

The total energy gained by the induction of dipoles, $E_p = \sum K_i z_i V_i^d / 2$, is -0.76 eV in La_2CuO_4 at $T = 10$ K. This is less than 0.4 % of the Coulomb energy, $E_C = \sum K_i z_i V_i^m / 2 = -195.4$ eV. In pyrite, the polarization energy was found to account for roughly 10% of the interaction energy of the ionic charges [31]. Regarding the energy parameter E, which is the binding energy if core-core repulsion, van der Waals interactions and energies due to thermal vibrations are neglected, $E = E_I + E_C + E_p = -71.44$ eV is obtained if all ionization energies of metal

and electron affinities of oxygen are collected in E_I. The error of E is solely determined by the inaccurate second electron affinity of oxygen. Applying (4) we also tried other charge assignments than the usual $(La^{3+})_2(Cu^{2+})(O^{2-})_4$, but never succeeded in finding a lower value for E. This charge assignment is therefore concluded to account for the minimum binding energy and to be consistent with respect to ionic and dipole potentials.

Since our goal was to compare different valence models, we opted not to consider the energy of repulsion E_r between the different ions. In many studies on heteropolar crystal, E_r was reported to amount approximately to 10% of the Coulomb energy, but of opposite sign [31, 34], $E_r \approx -0.1\, E_C$. The binding energy can be estimated if this rule of thumb is applied, and if energies due to van der Waals interaction and thermal vibrations are neglected, $E_{vdW} + E_{tv} \approx 0$. It is obtained $E_B = E + E_r \approx -50.5$ eV, but it should be remembered that this value gives only a very rough estimate of the binding energy of La_2CuO_4. Compared to this value, the polarization energy E_p amounts to 1.5% of the total binding energy.

We will now discuss electrostatic lattice sums and derived quantities of LSCO for $x \neq 0$. The data presented in Tables 6 and 7 have been distinguished for the three valency models if they depend on a certain assignment of charges, symbolized by M1, M2 and M3. This is the case for α^m and β^m coefficients and for the dipole moments μ, while α^d and β^d matrices are independent of the charges and are the same in all three models for constant x. Values of β^m were not given, because they can be calculated from these data with the help of (5). For $x = 0.21$ lattice sums of the type α^d_{ij}, β^d_{ij} and μ_j are not listed for $j = 1, 3, 5$, because they all vanish at the phase boundary. Some important quantities will be given as functions of the Sr concentration x in the figures as now being discussed.

In Fig. 2 the Coulomb potentials at the sites of metal and oxygen ions with increasing x are illustrated. In all cases, the calculated points can be well approximated by a straight line. We conclude that for $0 \leq x \leq 0.21$ the set of V_i^m may be expressed as linear functions of x. A comparison of the metal potentials reveals that with increasing doping the situation stated for La_2CuO_4 is reversed: whereas the incorporation of a charge $z = +3$ was found to stabilize the system if it occurs at the La site in La_2CuO_4, this no longer is valid for the full range of x. In all valency models a cross-over between V^m_{LS} and V^m_{Cu} can be identified between $0.01 < x < 0.04$, accounting consistently for the fact that two-fold positive charges (Sr^{2+}) are now being deposited on LS sites. Figure 2b shows the Coulomb potentials for the two oxygen sites. No cross-over can be observed, and we conclude that any depletion of electrons would be favoured energy-wise to occur at apex oxygen sites rather than at in-plane oxygens for the whole range of $x \geq 0$.

If the energy parameters E are solely calculated on the basis of the Coulomb potentials, symbolized by E^m in the following, the functions $E^m(x)$ as shown in Fig. 3a are found for the different models. According to the plot, model 1, which stands for the oxidation of Cu^{2+} ions, would be the one most favoured. But the differences between the three models would remain small, since there

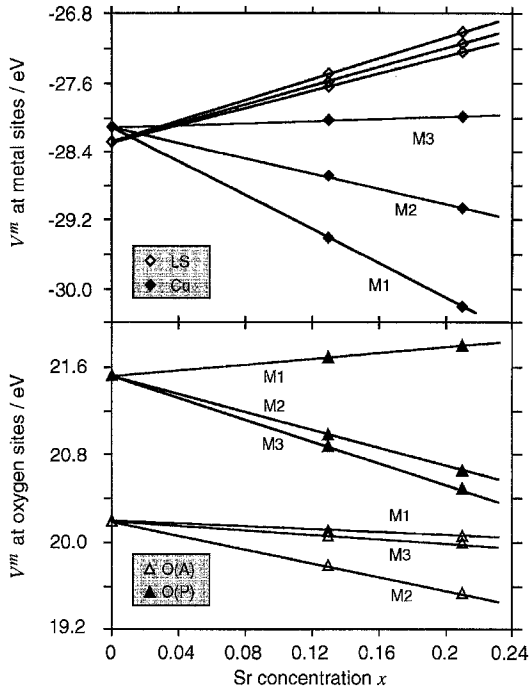

Fig. 2. Madelung potentials for (a) metal and (b) oxygen sites in $La_{2-x}Sr_xCuO_4$ at various Sr concentrations x and at $T \approx 16$ K. At $x = 0$ positive charges are more stable on LS sites than on Cu sites, but the situation reverses with increasing x for all valency models investigated (M1–M3). No cross-over is observed in the case of the two oxygen ions where electrons are favoured to be always located on O(P) positions. In this and all the following figures, straight lines connecting the calculated values at $x = 0, 0.13$ and 0.21 only serve as a visual guide

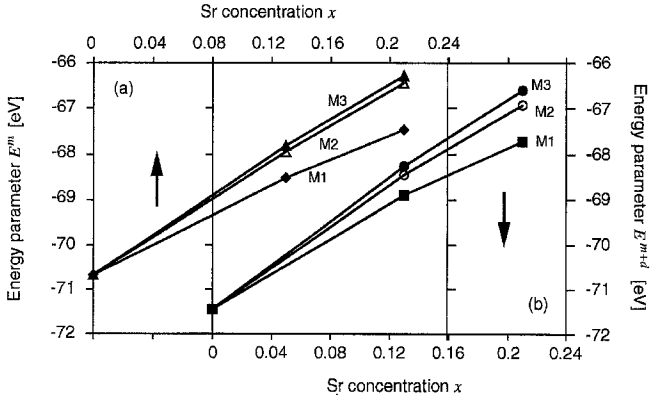

Fig. 3. Energy parameter E for the three valency models (a) excluding (E^m) and (b) including dipole shares (E^{m+d}). The differences between the E parameters are assumed to equal the differences of binding energies. Accordingly, model 1 that localizes the holes on copper sites is favoured in cases (a) and (b). However, the differences are very small, i.e. the binding energy of all models becomes closely spaced. Dipole contributions increase the binding energy of La_2CuO_4 by 0.76 eV, but the dipolar energy gain decreases with increasing x for each separate model

exists a delicate balance between the large amount of energy necessary to generate Cu^{3+} ions and the gain of energy due to increased Coulomb interaction. We will come back to this point with the discussion of the dipole energies.

The dipoles strengths $p_j(x)$ are shown for increasing Sr concentration for model 1 in Fig. 4. The set of $p_j(x)$ in the other models differ only slightly from the one presented and will not be discussed here. The main effect is the disappearance of the three dipoles p_b(LS), p_b(O(A)) and p_c(O(P)) at $x = 0.21$, which is remarkable in the case of p_b(LS), since it is the largest moment in La_2CuO_4. The p_c dipoles of LS and O(A) remain more or less constant over the whole range of doping investigated here. A recent work [13] states that the phase transition LTO → HTT at $x \approx 0.21$ may also be responsible for a vanishing critical temperature $T_c(x)$. Accordingly, three dipole components and superconductivity in $La_{2-x}Sr_xCuO_4$ would simultaneously disappear and a relation between both may be speculated. On the other hand, the existence of superconductivity was also reported in the tetragonal phase [35, 36], where the relevant dipole moments have disappered. For the time being, experimental data are concluded to be too controversial to correlate both phenomena.

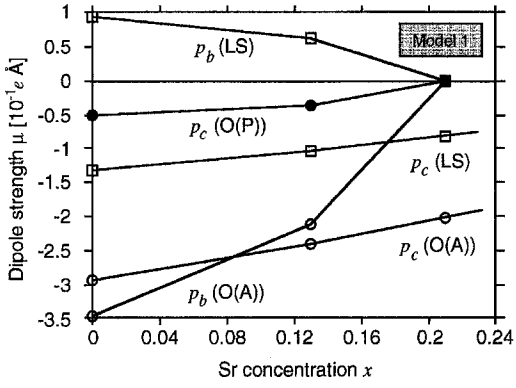

Fig. 4. Strengths of crystal field induced dipoles p_j in $La_{2-x}Sr_xCuO_4$ as calculated by electrostatic lattice coefficients of model 1. For $x = 0$ the dipole moment of O(A), $(p_b^2 + p_c^2)^{1/2} = 0.45$ eÅ, is larger than the moment of the water molecule of 0.38 eÅ. Three of five dipoles vanish during the phase transition at $x = 0.21$ including p_b(O(A)) which is the strongest component at $x = 0$. Only p_c components of LS and O(A) survive the phase transition LTO → HTT

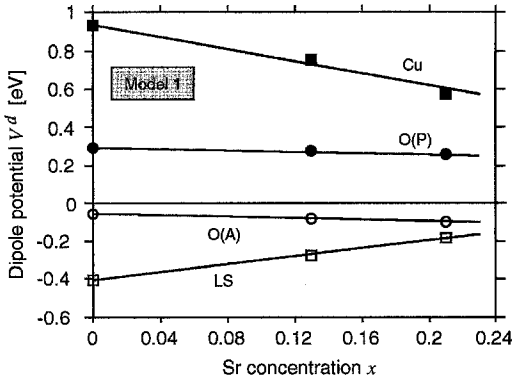

Fig. 5. Dipole potentials V^d for the different lattice sites in $La_{2-x}Sr_xCuO_4$ when holes introduced by doping are assumed to be associated with the copper ions (model 1). Except for O(A), the strength of all V^d decrease with increasing Sr concentration x which can be understood from the decline of dipole moments

Figure 5 shows the dipole potentials $V_i^d(x)$ for the four ions as they are obtained in model 1. We will not discuss the functions $V_i^d(x)$ within the other models, because they do not differ significantly. According to Fig. 5, except for $V_{O(A)}^d$ the strengths of all V_i^d decrease with increased doping, which is mainly caused by the diminution of three important dipole moments. But the set of V_i^d deviates from zero at the phase boundary and most probably beyond it, since the dipoles p_c(LS) and p_c(O(A)) also occur in the lattice of the HTT phase.

Figure 3b presents the energy parameter E with the inclusion of the polarization energy as a function of doping rate x. In comparison with E^m values the system is relaxed by approximately 0.25 to 0.75 eV in the different models. Consequently, the dipoles would increase the crystal binding. This result was to be expected according to the considerations in [10]. Again, model 1 is found to be favoured compared to models 2 and 3. This result is not influenced by the inaccuracy of the electron affinity of oxygen, which may only account for an error of approximately $\pm x$ eV in models 2 and 3 for Sr concentrations of x.

The decisive reason for model 1 being the most favoured one can be seen from Fig. 6a. The plot shows that the increase in $|V_{Cu}|$ is greatest in model 1. Because z_{Cu} also increases as $(2 + x)$ within this model, the energy gain of the system, $z_{Cu}V_{Cu}$, decreases quadratically with the Sr concentration. The inclusion of dipole potentials enhances this tendency compared to the situation where only

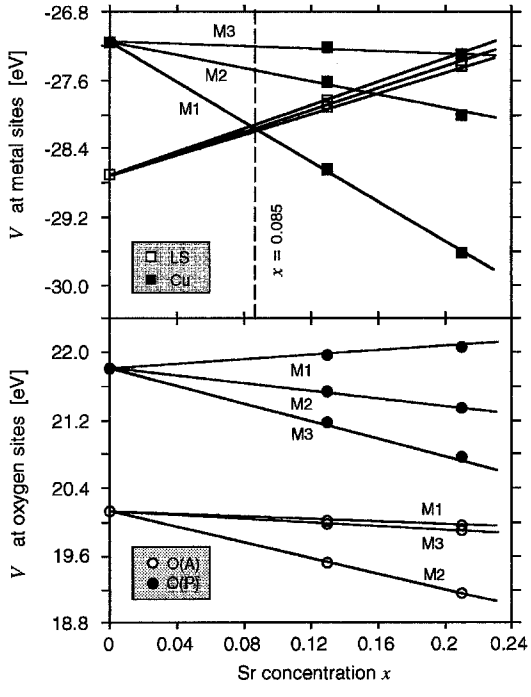

Fig. 6. Sums of Madelung and dipole potentials of the four ionic lattice sites of LSCO. The plot should be compared with Fig. 2, which shows only the monopole contribution of the crystal potential. Dipole potentials can be realized to have a significant effect when charge balances between different lattice sites are considered. The cross-over between V_{Cu} and V_{LS} in model 1 at $x = 0.085$ has been marked. The point is very close to the onset of superconductivity in this compound at $x \approx 0.06$

Coulomb potentials are considered. Also $z_{O(P)}V_{O(P)}$ can be seen from Fig. 6b to be a quadratically decreasing function for increasing x. The doping of La_2CuO_4 by Sr and the oxidation of Cu^{2+}, is concluded to modify mainly the crystal potentials of in-plane Cu and O(P). This modification of potentials increases the solid's binding energy more than any other charge assignments.

We have emphasized the point $x = 0.085$ in Fig. 6a, where again a cross-over of V_{Cu} and V_{LS} can be observed. For larger Sr concentration additional holes introduced into the solid become more stabilized on Cu sites than on LS lattice sites. The stoichiometry coordinate is remarkably close to $x = 0.06$, where superconductivity starts to occur in the phase diagram of LSCO [37].

The x-dependent difference of potentials $V_{O(A)} - V_{O(P)}$ and $V_{O(P)} - V_{Cu}$ may be extracted from Fig. 6 and from the tables. These expressions enter the Hamiltonian of the cluster model approach [1]. A comparison of Figs. 2 and 6 reveals that the parameter may change significantly when dipole potentials are included. It would be of great interest to know how the electronic structure calculated by the approach would vary if, next to the usual Madelung potentials, dipole effects were also taken into account. Also the plot of T_c over the difference of site potentials given by Ohta et al. [7] may significantly change after the addition of dipole potentials.

As we know, some investigators determined that the holes introduced by doping were also distributed over oxygen sites, see for instance [38]. These results seem hardly to be brought into line with this work favouring model 1, i.e. the depletion of electrons from the copper ions. However, the energy differences between the different models are very small. They range from 300 to 570 meV for $E_{M1} - E_{M2}$ at $x = 0.13$, for instance, depending on which value for the second electron affinity of oxygen is inserted. Therefore, an energy term that we have disregarded so far may bridge this gap, thereby favouring the system to be actually in a mixed state of all three models rather than solely in a state of model 1. Reference 17 argues that random crystal fields arise in such heterovalently substituted compounds as LSCO and give rise to random dipoles. The latter were shown to supply a further term to the binding energy. This terms and its influence on the competition between the different valency models will be investigated in a forthcoming work [39].

IV. Conclusions

For the first time, crystal-field induced dipoles in $La_{2-x}Sr_xCuO_4$ have been calculated as a function of varying Sr concentrations x. Five dipole components have been found to be induced in the orthorhombic phase of LSCO. Their number is reduced to two for the tetragonal compound. The strengths of the dipoles at $T \approx 16$ K amount to maximally 0.45 eÅ, being comparable to the dipole moment of the water molecule. The onsite dipole potentials were found to be in the range of a few percent of the Coulomb potentials and to increase the distinction between metal sites and oxygen sites, respectively. The polarization energy, however, was identified to be small and to account for roughly 1.5% of the total binding energy. Concerning the distribution of charges over the different lattice sites in $La_{2-x}Sr_xCuO_4$ the charging of copper ions according to $Cu^{2+} \rightarrow Cu^{3+}$ was shown to be the mechanism leading to the lowest binding energy of the system. However, a remarkable characteristic of the compound is that the energy used to introduce the holes (I_3(Cu) or A_2(O)) is almost perfectly outweighted by the energy gain due to changes of the crystal potentials. Because this rule holds true for all three valency models, their binding energies becomes almost equal. Regarding the high-T_c superconductivity of the compound, two remarkable points in the phase diagram have been revealed in this temperature range. First, a cross-over of the Cu and LS site potentials occurr near the onset of superconductivity at $x = 0.085$. Second, three regular dipole components vanish for $x = 0.21$, which coincides with the disappearance of superconductivity. Again, the electrostatic lattice coefficients have proven their usefullness for the understanding of structure and bonding in highly complex compounds. With their help it becomes possible to analyse the interaction between each sort of ion in a crystal lattice separately. This will be of importance whenever the properties of a compound are manipulated by doping with other ionic species.

One of us (MB) would like to thank W. Buckel, Karlsruhe, and M. Schmitz, hydronic GmbH, Bitburg, for very helpful discussions and their support of this work.

References

1. Maekawa, S., Ohta, Y., Tohyama, T.: in: Toshiba International School of Superconductivity (ITS^2), p. 29, Kyoto 1991. Maekawa, S., Sato, M. (eds.) Berlin, Heidelberg, New York Springer 1992
2. Kondo, J., Asai, Y., Nagai, S.: J. Phys. Soc. **57**, 4334 (1988)
3. Kondo, J.: in: Strong Correlation and Superconductivity p. 57, Mt. Fuji 1989, Fukuyama, H., Maekawa, S., Malozemoff, A.P. (eds.) Berlin, Heidelberg, New York: Springer 1989
4. Rushan, H., Zizhao, G., Daole, Y., Qing, L.: Phys. Rev. B **41**, 6683 (1990)
5. Cohen, R.E., Pickett, W.E., Krakauer, H., Boyer, LL.: Physica B **150,** 61 (1988)
6. Torrance, J.B., Metzger, R.M.: Phys. Rev. Lett. **63**, 1515 (1989)
7. Ohta, Y., Tohyama, T., Maekawa, S.: Phys. Rev. B **43**, 2968 (1991)
8. Wang, Q., Rushan, H., Gan, Z.Z.: Phys. Rev. B **45**, 10834 (1992)
9. Wright, N.F., Butler, W.H.: Phys. Rev. B **42**, 4219 (1990)
10. Birkholz, M.: Crystal-field induced dipoles I. Z Phys B **96**, 325 (1995)
11. Cava, R.J., Santoro, A., Johnson, D.W., Rhodes, W.W.: Phys. Rev. B **35,** 6716 (1987)
12. Braden, M., Schweiss, P., Heger, G., Schwarz, W., Wohlleben, D., Fisk, Z., Rumiantsev, A., Tanaka, I., Kojima, H.: Physica C **185–189**, 549 (1991)
13. Takagi, H., Cava, R.J., Marezio, M., Batlogg, B., Krajewski, J.J., Peck, W.F., Bordet, P., Cox, D.E.: Phys. Rev. Lett. **68**, 3777 (1992)
14. Jorgensen, J.D., Dabrowski, B. Pei, S., Hinks, D.G., Soderholm, L., Morosin, B., Schirber, J.E., Venturini, E.L., Ginley, D.S.: Phys. Rev. B **38**, 11337 (1988)
15. Braden, M., Schweiss, P., Heger, G., Reichardt, W., Fisk, Z., Gamayunov, K., Tanaka, I., Kojima, H.: Physica C **223**, 396 (1994), these authors specify the structural data in terms of the *Abma* setting of the unit cell

16. Torrance, J.B., Tokura, Y., Nazzal, A.I., Bezinge, A., Huang, T.C., Parkin, S.S.P.: Phys. Rev. Lett. **61**, 1127 (1988)
17. Birkholz, M.: Crystal-field induced dipoles II. Z. Phys. B **96**, 333
18. Fraga, S., Karwowski, J., Saxena, K.M.S.: Handbook of atomic data, Table VI (1). Amsterdam: Elsevier 1976
19. Tessman, J.R., Kahn, A.H., Shockley, W.: Phys. Rev., **92**, 890 (1953)
20. Pauling, L.: Proc. Roy. Soc. **114A**, 181 (1927)
21. Jain, S.C., Sharma, T.P., Arora, N.D.: J. Phys. Chem. Solids **37**, 81 (1976)
22. Shanker, J., Argrawal, G.G, Dutt, N.: Phys. Statis. Solid: (b) **138**, 9 (1986)
23. Dikshit, U.C., Kumar, M.: Phys. Statis Solid. (b) **165**, 559 (1991)
24. Radzig, A.A., Smirnov, B.M.: Reference data on atoms, molecules and ions, p. 131. Berlin, Heidelberg, New York: Springer 1985
25. Cotton, F.A., Wilkinson, G.: Advanced inorganic chemistry, p. 58. New York: Wiley 1972
26. Ashcroft, N.W., Mermin, N.D.: Solid state physics, p. 673. Tokyo: CBS 1981
27. Loram, J.W., Mirza, K.A.: in: Electronic properties of high-T_c superconductors and related compounds. Kirchberg, Tyrol 1990, p. 92, Kuzmany, H., Mehring, M., Fink, J. (eds.). Berlin, Heidelberg, New York: Springer 1990
28. Evjen, H.M.: Phys. Rev. **15**, 675 (1932)
29. Marathe, V.R., Lauer, S., Trautwein, A.X.: Phys. Rev. B **27**, 5162 (1983)
30. Rudert, R., Birkholz, M.: ELC – a computer program for the calculation of electrostatic lattice coefficients 1994
31. Birkholz, M.: J. Phys.: Condensed Matter **4**, 6227 (1992)
32. Nelson, R.D., Lide, D.R., Maryott, A.A.: in: Handbook of chemistry and physics, p. E-61, Weast, R.C. (ed.) Boca Raton: CRC Press 1986
33. Brumer, P., Karplus, M.: J. Chem. Phys. **58**, 3903 (1973)
34. Weiss, A., Witte, H.: Kristallstruktur und chemische Bindung, p. 122. Weinheim: Verlag Chemie 1983
35. Torrance, J.B., Bezinge, A., Nazzal, A.I., Huang, T.C., Parkin, S.S.P., Keane, D.T., LaPlaca, S.J., Horn, P.M., Held, G.A.: Phys. Rev. B **40**, 8872 (1989)
36. Schäfer, W., Breuer, M., Bauer, G., Freimuth, A., Knauf, N., Roden, B., Schlabitz, W., Büchner, B.: Phys. Rev. B **49**, 9248 (1994)
37. Shafer, M.W., Penney, T., Olson, B.L.: Phys. Rev. B **36**, 4047 (1987)
38. Pellegrin, E. et al.: Phys. Rev. B **47**, 3354 (1993)
39. Birkholz, M., Rudert, R.: Z. Phys. B (forthcoming)